Conference paper

María Angélica Gómez, Jennifer Marcela Bonilla, María Alejandra Coronel, Jonathan Martínez, Luis Morán-Trujillo, Sandra L. Orellana, Alejandra Vidal, Annesi Giacaman, Carlos Morales, César Torres-Gallegos, Miguel Concha, Felipe Oyarzun-Ampuero, Patricio Godoy, Judit G. Lisoni, Carla Henríquez-Báez, Carlos Bustos and Ignacio Moreno-Villoslada*

Antibacterial activity against *Staphylococcus aureus* of chitosan/chondroitin sulfate nanocomplex aerogels alone and enriched with erythromycin and elephant garlic (*Allium ampeloprasum L. var. ampeloprasum*) extract

https://doi.org/10.1515/pac-2016-1112

Abstract: The antibacterial activity against *Staphylococcus aureus* of aerogels fabricated from colloidal suspensions of chitosan/chondroitin sulfate nanocomplexes is analyzed. Upon freeze-drying the colloidal suspensions, the aerogels presented a porous structure made of microsheets and microfibers. The aerogels could, in addition, be loaded with antimicrobial agents. Loaded with the antibiotic erythromycin, the aerogels showed crystalline deposits, affecting the topography of the samples as well as their mechanical properties, showing a decrease on the apparent Young's modulus and hardness at 40 % deformation. Loaded with elephant garlic (*Allium ampeloprasum L. var. ampeloprasum*) extract, the aerogels showed texturization of the microsheets and microfibers, and the higher relative mass allowed an increase on the apparent Young's modulus and hardness at 40 % deformation with respect to pristine aerogels. Unloaded aerogels showed activity against *Staphylococcus aureus*, including a methicillin-resistant strain. The release of erythromycin from the aerogels to an agar environment is governed by equilibrium forces with the polysaccharides, which allow modulating the load of antibiotic and its concomitant diffusion from the material. The diffusion of the active components of the elephant garlic extract did not show a dependence on the polysaccharide content, revealing a week interaction. The elephant garlic extract resulted active against the methicillin-resistant *Staphylococcus aureus* strain, while resistance was found for the antibiotic, revealing the therapeutic potential of the natural extract. The antimicrobial aerogels may be used for several therapeutic purposes, such as healing of infected chronic wounds.

Keywords: antibacterial materials; antibiotic erythromycin; elephant garlic; ICCC-13; polysaccharide-based aerogels; wound care.

Article note: A collection of invited papers based on presentations at the 12th Conference of the European Chitin Society (12th EUCHIS)/13th International Conference on Chitin and Chitosan (13th ICCC), Münster, Germany, 30 August–2 September 2015.

***Corresponding author: Ignacio Moreno-Villoslada,** Instituto de Ciencias Químicas, Facultad de Ciencias, Universidad Austral de Chile, Isla Teja, Casilla 567, Valdivia, Chile, Tel.: +56 63 2293520, E-mail: imorenovilloslada@uach.cl

María Angélica Gómez, Jennifer Marcela Bonilla, María Alejandra Coronel and Jonathan Martínez: Facultad de Ciencias de la Salud, Universidad Colegio Mayor de Cundinamarca, Bogotá, Colombia

Luis Morán-Trujillo, Sandra L. Orellana, Carlos Morales, César Torres-Gallegos and Carlos Bustos: Instituto de Ciencias Químicas, Facultad de Ciencias, Universidad Austral de Chile, Valdivia, Chile

Alejandra Vidal, Annesi Giacaman and Miguel Concha: Instituto de Anatomía, Histología y Patología, Facultad de Medicina, Universidad Austral de Chile, Valdivia, Chile

Felipe Oyarzun-Ampuero: Department of Sciences and Pharmaceutical Technologies, Universidad de Chile, Santiago, Chile

Patricio Godoy: Instituto de Microbiología Clínica, Facultad de Medicina, Universidad Austral de Chile, Valdivia, Chile

Judit G. Lisoni and Carla Henríquez-Báez: Instituto de Ciencias Físicas y Matemáticas, Facultad de Ciencias, Universidad Austral de Chile, Valdivia, Chile

Introduction

Tissue engineering provides new alternatives for the repair or regeneration of damaged tissues. In particular, skin regeneration is essential in human health due to the importance of this organ as a physical barrier to pathogens, and the social and psychological problems associated to damaged skin. Chronic wounds such as diabetic foot and venous ulcers may require the use of dermal substituents and functional dressings that favor wound healing. Several biodegradable and non-toxic architectures have been designed for scaffolds as wound dressings [1–4]. In addition, diabetic foot ulcers, abscess, venous ulcers, pressure ulcers, acne, cellulitis, impetigo, and dermatitis are found among diseases that may produce infections, further complications, and permanent lesions and scars. Infections in wounds and skin lesions produce a slow-down on the rate of healing, and a risk of systemic propagation. Treatment of infected lesions could involve changes on the patient diet, the use of skin protectors from sunlight and other external agents, and therapy with antibiotics.

Skin and soft tissue infections are a frequent cause of consultation in hospital services. Their etiologic diagnosis and antibiotic treatment highly depend on the epidemiological context of the infection [5–8]. Etiologic agents most frequently isolated in these infections are Gram-positive aerobic bacteria, in most cases *Staphylococcus aureus* (*S. aureus*) [5–9]. *S. aureus* is a bacteria of the *Micrococcaceae* family, part of the normal flora of human skin and mucous, and asymptomatically colonizes approximately a third of the population [10]. *S. aureus* is, however, potentially pathogenic, able to colonize certain areas of the skin and mucous membranes, having particular virulence mechanisms [11]. In the last two decades *S. aureus* has emerged as a predominant etiological agent of community-associated skin and soft tissue infections [12, 13]. It is considered the main etiologic agent of hospital-acquired (nosocomial) skin infections and the most common cause of infection in surgical incisions. It causes suppurative infections and toxinoses in humans, superficial skin lesions as furuncles and styes, and more serious systemic infections [14]. Rapid adaptation of *S. aureus* to environmental changes allows efficient spreading in the environment, infecting other patients in hospitals and the community outside clinical centers. Methicillin-resistant *Staphylococcus aureus* (MRSA) were discovered in the 1960s and became a pathogen in several hospitals around the world. Later, strains of MRSA outside the hospitals, known as community-associated MSRA, emerged causing skin and soft tissue infections, as reported in the 1980s and the 1990s [15, 16]. Associated epidemiological changes on *S. aureus* and its related diseases may require new strategies for antibiotic treatment [17].

Recently, we have developed aerogels based on microfibers and microsheets made of chitosan (CS) and chondroitin sulfate (ChS). These aerogels were engineered as wound healing inductors, based on three strategies: (1) provide a minimum amount of matter to be applied in order to avoid additional metabolic stress to the wounds, impairing healing, and production of excessive debris and other by-products of metabolism, (2) provide low electrostatic potential avoiding disruption of the cellular membrane integrity, and induction of extensive inflammatory response [18], and (3) provide physiological functionality rather than constitute scaffolds for cell attachment and growing. Thus, aerogels have been synthesized with density ranging between 10^0 and 10^1 mg/cm^3 that combine the biological properties of both CS and ChS [19, 20] and contain equimolar amounts of both complementary charged polymers (considering moles of ionizable groups), avoiding covalent cross-linking and the use of any organic solvent. The aerogels have been shown to be angiogenic, and, applied to skin lesions, to improve the quality of the dermal tissue, with suppression of pain and bad smell, accelerating wound healing in diabetic foot and venous ulcers [21]. Their mechanical properties facilitate their application in open wounds, easily adapting to the wound contour due to their malleability. Once applied to the wounds the material swallows and hydrates, so that it does not need to be removed, since is physiologically degraded. In addition, it can be easily compressed, sterilized, and packed in appropriate containers, facilitating their storage and transportation, conditions necessary for their commercialization and clinical management.

Another advantage of the designed aerogels is that they can be used as carriers of different molecules such as drugs, nutrients, etc. Since infections in skin lesions, in particular in chronic ulcers, jeopardize the adequate healing, in this paper we will analyze the behavior of ultralight, highly porous CS/ChS aerogels against two *S. aureus* strains, including sensitive and resistant (MRSA) strains. In addition, we will show

the fabrication and characterization of aerogels loaded with antibacterial substances, such as the antibiotic erythromycin (ERY) and an aqueous extract of elephant garlic (*Allium ampeloprasum L. ampeloprasum*), and their antibacterial activity will be analyzed.

Experimental

Materials

CS (Protasan™ UP CL 213, Novamatrix, 83 % deacetylation, MW of 239.22 g/mol of amino units considered), ChS (Chondroitin sulfate A sodium salt from bovine trachea, Sigma-Aldrich, MW of 252 g/mol of ionizable groups considered), ERY (Sigma-Aldrich, MW of 734 g/mol, pK_a = 8.7), and an aqueous extract of elephant garlic, whose main active component is allicin [22], have been used to prepare the solid materials. The molecular structures are shown in Fig. 1. ERY Sensi-Discs™ (ESD) of 6 mm of diameter containing 15 µg (0.02 µmol) of ERY (Valtek S.A.) were used for biological assays. A 0.5 scale McFarland Nephelometer Standar (BD BBL™) was used to compare and adjust suspended inoculums of *S. aureus* strains. A 5000 MW cut-off cellulose ultrafiltration membrane was used for elephant garlic extract ultrafiltration.

Bacterial strains

The antibacterial properties of the fabricated aerogels were tested against two bacterial isolates: a reference strain consisting of *S. aureus ssp. aureus* (American Type Culture Collection [ATCC] no. 25923), and a clinical isolate of MRSA from a patient at the hospital. All strains were stored and made part of the ceparium at the *Universidad Austral de Chile* (*Instituto de Microbiología Clínica*). The clinical isolates were identified by

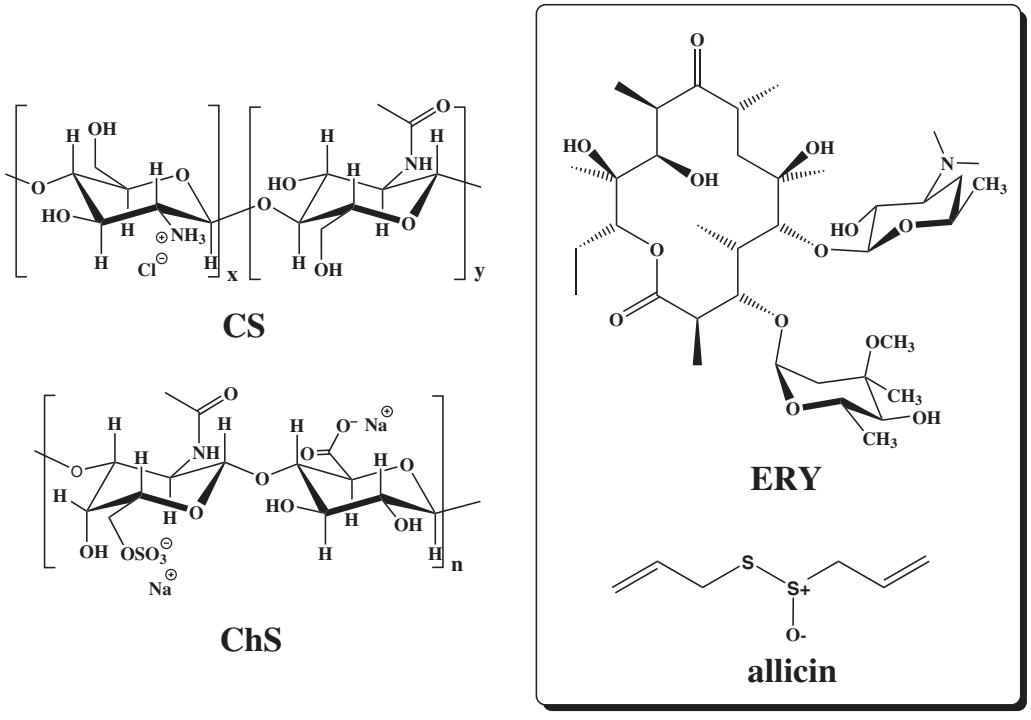

Fig. 1: Molecular structures of CS, ChS, ERY, and allicin.

routine laboratory methods, Gram's method, coagulase test, mannitol fermentation, and urease test. The antibiotic sensitivity of both clinical strains was tested by the Kirby Bauer [23] method using gentamicin, ciprofloxacin, oxacillin, trimethoprim sulfamethoxazole, linezolid, clindamicin, lincosamide, and ERY and resistance of the MRSA strain to ERY was corroborated.

Equipment

A XB 120 A balance (Precisa) was used to weight the reactants, and corresponding solutions were prepared in water deionized in a Simplicity (Millipore) deionizer. The pH of the solutions was measured with a Scholar 425 pH meter (Corning). An orbital shaker (WiseCube) was used to macerate extracts of elephant garlic in deionized water. The aqueous extracts were separated from remaining solid particles by ultrafiltration over a regenerated cellulose membrane of nominal molecular weight cut-off of 5000 Da (Millipore) placed in a 10 mL ultrafiltration cell (Amicon). The system was subjected to three bar by the aid of N_2 99.995 % (AGA). A 75900-55 perfusion pump (Cole-Parmer Instrument Co.) was used to mix stock solutions of CS and ChS under stirring with a MR1000 magnetic stirrer (Heidolph). Apparent size and zeta potential of particles in the resulting CS/ChS colloidal suspensions were measured by dynamic light scattering (DLS) with a zetasizer Nano ZS equipment (Malvern). The particle size polydispersion index (PDI) is calculated from the DLS data as the square of the size relative standard deviation [24]. Freeze-drying was carried out in an Alpha 1–2 LD plus lyophilizer (Christ). Scanning transmission electron microscopy (STEM) images were obtained in an Inspect 50 (FEI) instrument. Optical pictures were taken with an iPhone 5C mobile phone equipped with an 8 megapixels camera or with a Nikon D3000 camera. The mechanical properties were characterized in a CT3 1000 Texture Analyzer (Brookfield) controlled with the TexturePro CT3 software (Brookfield). The aerogels were sterilized by UV radiation in a Purifier Class II laminar flux cabinet (Labconco). Bacteria were grown in a CO_2 incubator (Shellab).

Procedures

Stock solutions preparation

A 2×10^{-3} M solution (25 mL) of ERY was prepared by dissolving 0.037 g in deionized water at pH 3. The solution was stored at 4 °C. The elephant garlic aqueous extract was prepared from peeled and crushed fresh cloves of elephant garlic (25 g) using a mortar and a pestle, homogenizing with 25 mL of deionized water at pH 5.0. The resulting mixture was allowed to macerate under stirring for 1 h at 220 rpm at 20 °C in a 100 mL glass beaker. The obtained mixture was ultrafiltered over a 5000 MW cut-off cellulose membrane, and the filtrate was stored frozen at –15 °C to avoid allicin decomposition [25, 26], if necessary. CS stock solutions have been prepared by dissolving 0.059 g in 25 mL of deionized water at pH 5.0. Prior to CS stock solution preparation, CS powder was dried in an oven for 4 h at 100 °C. ChS stock solutions have been prepared by dissolving 0.063 g in 25 mL of deionized water at pH 5.0. Both polymeric stock solutions were prepared at a concentration of 1×10^{-2} mol of polymeric ionizable groups per liter.

Colloidal suspensions preparation

Freshly prepared stock solutions of CS and ChS were placed in 20 mL plastic syringes. Using a perfusion pump, 4 mL of each of the polymer stock solutions were simultaneously added drop wise to a flask containing 10 mL of deionized water at 20 °C and pH 5.0, at a flux of 880 μL min^{-1}, and gently stirring with a magnetic stirrer. Alternatively, the addition of the stock solutions was done with the aid of micropipettes, adjusting the volumes to a desired final absolute and relative concentration of the polysaccharides. After the biopolymers have been mixed producing a milky suspension, ERY or elephant garlic extract was added. In order to incorporate ERY in

the suspensions, 2 mL of different mixtures of water and ERY stock solution were added to the mixture, achieving different final ERY concentrations (method 1). Alternatively, the biopolymers were added to the container containing variable and less than 10 mL of water, and aliquots of the ERY stock solution were then added to complete a total volume of the colloidal suspensions of 18 mL (method 2). Elephant garlic extract was incorporated following a method similar to the method 2 for the incorporation of ERY: 4.56 mL of ChS and 3.44 mL of CS stock solutions were added drop wise to 1.72, 9.16, and 9.64 mL of deionized water at pH 5.0, and then 8.28, 0.84, and 0.36 mL of elephant garlic aqueous extract with the pH adjusted to 5.0 were, respectively, added to the mixture, in order to obtain three colloidal suspensions with the same apparent concentration of the polysaccharides and different concentration of the elephant garlic extract. The colloidal suspensions were characterized by STEM and analysis of apparent particle size, size PDI, and zeta potential. STEM images were obtained by sticking a droplet (10 µL) of the nanoparticle suspension on a copper grid (200 mesh, covered with Formvar) for 2 min, then removing the droplet with filter paper avoiding the paper touching the grid, then washing twice the grid with a droplet of Milli-Q water for 1 min, and removing the droplet with filter paper. Later, the sample was stained with a solution of 1% phosphotungstic acid by sticking a droplet of this solution on the grid for 2 min and removing the droplet with filter paper. Finally, the grid is allowed to dry for at least 1 h before analysis.

Aerogel formation

After the colloidal suspensions were formed, 200 µL, 2 mL, and 4.0 mL were transferred to 12×8 cm^2 wellplates of 96, 24, and 6 wells, respectively. The internal diameters of the respective wells were 7, 16, and 35 mm. In the case of the aerogels containing elephant garlic extract, due to the high mass of the extract, volumes of 150 µL, 1.5 mL, and 3.5 mL of the three colloidal suspensions obtained before were, respectively, added to the different wells. The volumes and apparent concentration of the garlic extract were chosen in order they represent 46.6, 4.66, and 2% of the total volume, so that the absolute amount of added extract is equivalent in the three aerogels formed in the different wells (70 µL). The samples were frozen at –15 °C for 24 h, and then freeze-dried at 0.050 mbar for 72 h, and a temperature of the condenser of –57 °C. If necessary, the resulting aerogels were stored at 4 °C in closed containers containing dried silica gel, in order to avoid moisture. SEM analyses were performed after coating the samples with a layer of gold atoms. Mechanical characterizations of aerogels of around 12 mm of diameter were performed in the compression mode, and the hardness and apparent Young's modulus (E_{app}) were obtained. The aerogels were fitted on a fixture base table (TA-BT-KIT, Brookfiled), and compressed, carefully centered, with a cylindrical TA-10 probe of 12.7 mm of diameter. The resolution of the texture analysis system was 0.1 g and 0.1 mm. The test speed was set at 0.7 mm s^{-1}, the load trigger value ranged from 0.7 to 1.0 g, and the maximum load was set at 12 g. For the final E_{app} analysis, data corresponding to deformations ranging between 30 and 50% are considered.

Anti-microbial tests

Mueller-Hilton Agar (MHA) plates were prepared by dissolving 38 g of MHA in a flask containing one liter of distilled water, then sterilizing at 121 °C and cooling down to ~45 °C. Approximately 20 mL of the prepared MHA were added into pre-sterilized Petri plates and let gelate. The antimicrobial activity against *S. aureus* strains of 5, 12, and 30 mm of diameter CS/ChS-based aerogels, loaded or not loaded with ERY or elephant garlic extract, was tested using the modified Kirby-Bauer Disk diffusion test protocol performed according to the guidelines of the Clinical and Laboratory Standards Institute (CLSI) [27, 28]. Inoculums were prepared by suspending 3–5 colonies of the pure strain of *S. aureus* of similar appearance with the aid of a sterilized loop in a test tube of saline solution. The colonies were obtained from a primary culture plate previously incubated in non-selective blood agar for 24 h. The number of colonies added were adjusted until achieving a turbidity approximately of 0.5 McFarland Nephelometer Standard scale ($1–2 \times 10^8$ CFU/mL), in an optimal time of 15 min. The adjusted suspension of bacteria were then inoculated to the MHA plates with a sterile swab

streaking the swab over the surface of the MHA medium three times rotating the plate approximately 60° in each application, then over the internal edge of the plate, and finally leaving the plate to dry for few minutes at room temperature with the lid closed. Prior to test the susceptibility of *S. aureus* to the new materials, the aerogels were submitted to UV-radiation, and transferred from the well-plates to the inoculated MHA plates. ESD and aqueous extract of elephant garlic (70 µL) were used as positive controls. Minimum inhibitory concentration of elephant garlic extract was studied by the macrodilution test [29]. Serial dilutions (consecutive dilution factor of 2) of the pristine extract in Tryptose broth (Merck 110676) were done in test tubes of 10 mL, so that 0.9 mL of the successive dilutions were contained in the test tubes to which 0.1 mL of a bacterial suspension of 1.5×10^8 CFU/mL were added. The elephant garlic positive control was placed on circular wells of 6 mm of diameter cut on the agar culture media. The bacterial cultures stood for 24 h at 35 °C in the presence of the samples. The results presented are the average of at least three trials per composition tested.

Results and discussion

Pristine aerogels

The starting point to produce the aerogels is the formation of colloidal suspensions of CS/ChS interpolymer nanocomplexes in aqueous medium, without needing covalent crosslinkers [30]. Stock solutions of both complementary charged polyelectrolytes were mixed in water so that ionic self-assembly easily occurs, due to the large amount of charges in every single molecule. Adjusting the stoichiometry to a 1:1 molar ratio of polymeric ionizable groups, thus achieving a high degree of electroneutralization between polymer charges, the mixture easily undergoes precipitation. In order to avoid this, the addition protocol involves careful control of the pH, simultaneous drop wise addition of both stock solutions, and moderate maximum final apparent concentration of both polymers (4.44×10^{-3} M). This provides a simple method of production of colloidal particles with apparent sizes falling in the nanometer range that does not involve toxic molecules. Then, by simultaneously pouring the CS and ChS stock solutions in a flask containing water, following the methodology described in the experimental part, colloidal suspensions of equimolar amounts of both polysaccharides were obtained, showing a particle mean apparent hydrodynamic diameter of 352 ± 32 nm and a mean zeta potential of 38 ± 2 mV ($n=11$). The size PDI values found were as low as 0.19 ± 0.03, reflecting a monomodal distribution of the particles. The final pH of the colloidal suspensions remained almost at 5.0, so that partial protonation of the carboxylate units of ChS allowed an excess of positive polymer charges furnished by CS, which produces a positive zeta potential, high enough to ensure stability of the nanoparticles in water, since electrostatic repulsions minimize particle aggregation. STEM images of the nanoparticles formed can be seen in Fig. 2a. The particles showed spherical shape with diameters of around 320 nm, very similar to those found

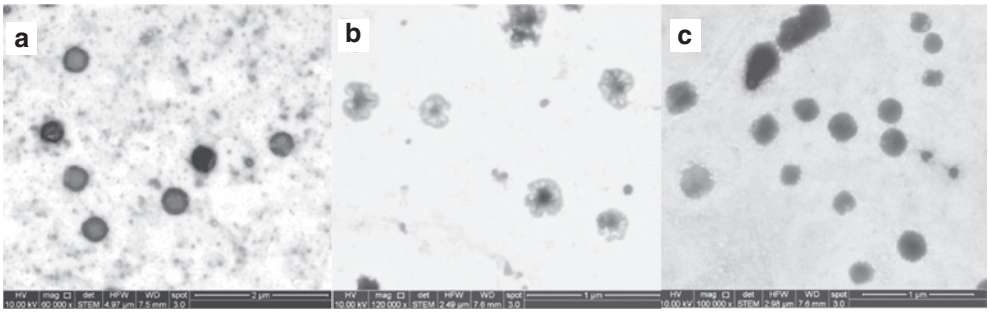

Fig. 2: STEM images of the nanoparticles obtained after mixing (a, 6×10^4 X) CS and ChS at a molar ratio 1:1, (b, 12×10^4 X) CS and ChS at a molar ratio 1:1 and ERY at a relative concentration of 0.023 mol of ERY/mol of polymeric ionizable groups, and (c, 12×10^4 X) CS and ChS at a molar ratio 0.75:1 and 4.66 % (v/v) of elephant garlic extract.

by DLS, indicating that the highly neutralized particles are scarcely hydrated and behave as solid polymeric nanoparticles more than as hydrated aggregates.

Volumes of 0.2, 2.0, and 4.0 mL of colloidal suspensions were placed in wells of 5, 12, and 30 mm of diameter. Upon solvent removal from the CS/ChS interpolymer nanocomplex suspensions by freeze-drying, a solid material arises due to the cohesive forces between particles. During freezing the colloidal suspensions, the nanometric particles are concentrated at the boundary of ice crystals being forming, submitted to the so-called "*ice-segregation-induced self-assembly*" (ISISA) [31–33]. Electrostatic interactions between the complementary charged chains of CS and ChS and their rigidity enhance the cohesive forces between particles, allowing obtaining well-structured porous materials. Thus, porous aerogels of different size and mass have been obtained with this methodology, as can be seen in Fig. 3a–c and Table 1. The sugar-cotton-like porous structures presented irregular shapes, with diameters slightly lower than the wells they were produced in, as can be read in Table 1. They are low-dense, soft materials, with total mass of 0.22, 2.2, and 4.4 mg for aerogels of 5, 12, and 30 mm of diameter, respectively. The density of the aerogels may vary according to the dimensions of the container and the volume of liquid added. Thus, aerogels of 30 mm resulted less dense, i.e. more porous, since the liquid volume in the cylindrical container spreads more in the x/y plane than along the z axis, compared with the wells of 5 and 12 mm of diameter. During the sublimation step, the materials expand in the z axis. SEM images of the materials show that they are composed of microsheets and microfibers presenting a smooth surface, as can be seen in Fig. 4. E_{app} of around 2 kPa and hardness of around 12 g at 40 % deformation has been found by texture analyses for aerogels of 12 mm of diameter.

The antimicrobiological properties of the aerogels were analyzed in cultures of two different strains of *S. aureus*, including a sensitive reference strain and a MRSA strain. After placing the aerogels on agar plates,

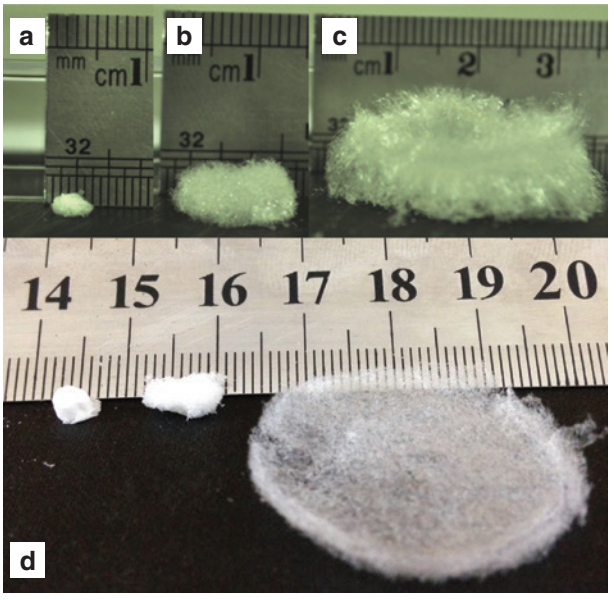

Fig. 3: CS/ChS-based aerogels of 5 (a), 12 (b), and 30 (c) mm of diameter with no additives, and with around 7.5 mg of elephant garlic extract (d).

Table 1: Physical characteristics of average CS/ChS-based aerogels.

Well diameter (mm)	Aerogel diameter (mm)	Total mass (mg)	Aerogel height (mm)	Density (mg/cm³)
7	5	0.22	2–3	3.7–5.5
16	12	2.2	3–6	6.4–3.1
35	30	4.4	8–12	0.8–1.2

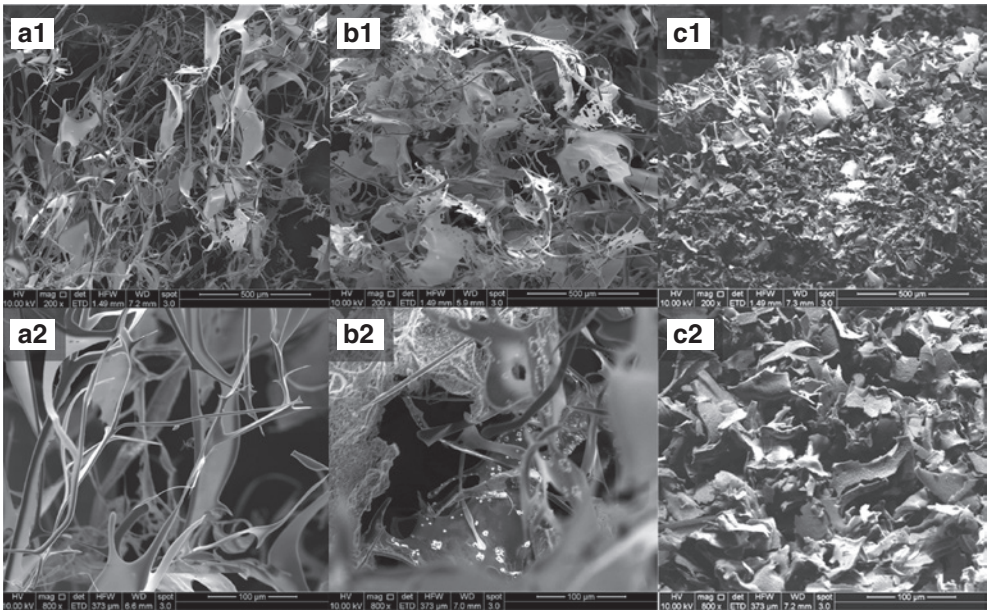

Fig. 4: SEM images of aerogels composed of CS and ChS in the absence of any additive (a) and in the presence of a relative amount of ERY of 0.023 mol of ERY/mol of polymeric ionizable groups (b), and in the presence 82 wt.% of elephant garlic extract (c) at two different magnifications: 200× (1) and 800× (2).

they swell and hydrate, forming a hydrogel on the agar substrate, which may potentially be colonized by the bacteria. ESD positive controls produced inhibition zone diameters (IZD) of 26 ± 3 mm (n = 20) in cultures of sensitive *S. aureus*, as can be seen in Fig. 5a, where a single assay is presented as reference, but did not produce inhibition haloes on MRSA cultures, as can be seen in Fig. 5b and c. It can be also seen that both the sensitive and the resistant bacteria did not grow in the zone occupied by the swollen aerogels of different size. CS has known antifungal and antibacterial effects [34] that are transferred to derived materials such as CS films [35]. This is attributed to its polycationic nature [36]. It is reported in the literature that CS does not diffuse on the agar gel [37], and our results support this statement, since no inhibition is found beyond the limits of the swollen aerogels.

Aerogels loaded with ERY

The strategy to load ERY to CS/ChS aerogels aimed at incorporating the antibiotic in the colloidal suspension prior to freeze-drying. In order to find the best fabrication protocol for the incorporation of ERY in the colloidal

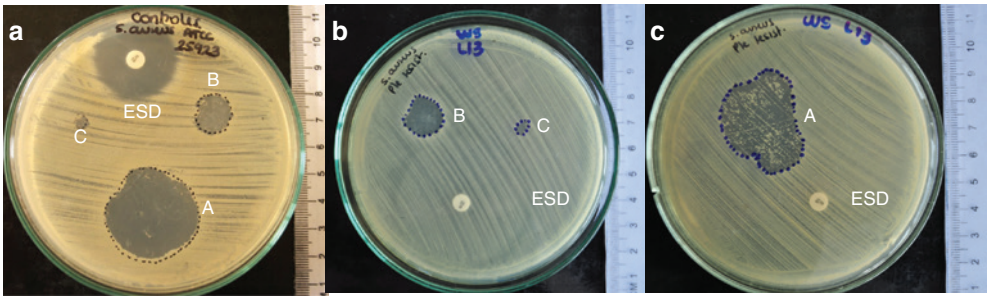

Fig. 5: Susceptibility test of ESD and aerogels of 30 (A), 12 (B), and 5 (C) mm of diameter on ATCC 25923 standard *S. aureus* (a) and MRSA (b and c) strains.

suspensions different methodologies have been tested. When ERY was added to the aqueous mixture in the container previous to the addition of the polymeric stock solutions, instability of the final mixture was found, probably caused by the low pH at which ERY must be dissolved, and macroprecipitates appeared. Then, we decided to add ERY immediately after the CS/ChS colloidal suspensions were formed, to the same container, and at the same stirring speed and flux. In this case, complexation between the polymers furnishes stability of the colloidal suspension during the addition of ERY, so that no macroprecipitation was observed with this methodology. An example of the nanoparticles formed can be seen in Fig. 2b. STEM images showed nanoparticles of around 300 nm with a different structure when comparing to the pristine CS/ChS nanocomplexes, since a dense core can be observed in the nanoparticles, coated by aggregates that form a hollow shell.

To fabricate series of aerogels with different amounts to ERY, two methodologies of addition of ERY after the CS/ChS nanoparticles are formed may be applied. If the range of ERY amount to be loaded is low, requiring low volumes of ERY stock solutions, it is useful to prepare the CS/ChS colloidal suspensions in a fixed volume, obtaining submicroparticles produced at comparable conditions, and then add a small fixed volume of ERY at different concentrations. However, if the range of ERY amount to be loaded is high, requiring high volumes of ERY stock solutions, it is more convenient to prepare the CS/ChS colloidal suspensions in variable volumes, achieving a final constant volume with the aid of a concentrated ERY stock solution, avoiding excessive dilution of the nanocomplexes. These two methodologies are reported in the experimental sections as method 1 and method 2, respectively. In order to check the influence of the incorporation of large amounts of ERY by the method 2 on the particle properties, the apparent size and zeta potential of the particles formed is analyzed. It can be seen in Fig. 6 that as the amount of ERY to be incorporated increases, the apparent size increases, and the zeta potential of the particles slightly increases. This effect may be caused by the higher final apparent concentration of the polyelectrolytes before adding increasing volumes of ERY, and also by slight changes in the pH when adding ERY, or by effective interactions of the antibiotic with the polymers, affecting molecular aggregation.

After freeze-drying the colloidal suspensions containing ERY, the aerogels formed did not show significant changes on the macroscopic dimensions and porosity as compared with the case in the absence of the antibiotic, due to the low relative mass of the antibiotic, and the role of the polysaccharides as the main structural components (pictures not shown). However, SEM images of aerogels of 12 mm of diameter loaded with 0.2 μmol of ERY, which represent a relative amount of 0.023 mol of ERY/mol of polymeric ionizable groups, presented a holey structure on the microsheets. In addition, deposits of microcrystals of ERY and/or NaCl and texturization on the microsheet surface were observed (Fig. 4b). This lowers the hardness of the aerogels, which decreased to a minimum of approximately half the value in the absence of the antibiotic, i.e. around 5.4 g at 40 % deformation, at a relative amount of ERY of 0.009 mol of ERY/mol of polymeric ionizable groups.

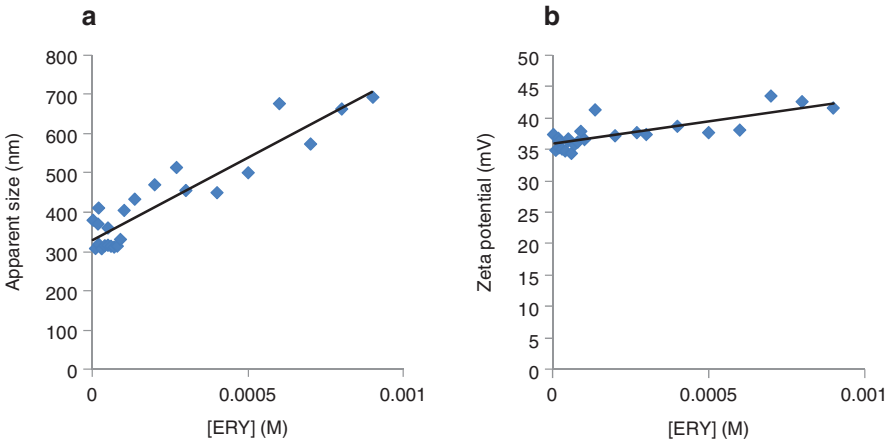

Fig. 6: Apparent hydrodynamic diameter (nm) (a) and zeta potential (b) of colloidal suspensions of CS/ChS containing different amounts of ERY, as a function of the ERY final concentration, obtained by the method 2.

The E_{app} found for the aerogel containing a relative amount of 0.023 mol of ERY/mol of polymeric ionizable groups decreased as compared with the pristine aerogel, achieving a value around 1.4 kPa.

The antibacterial activity of aerogels containing 0.02 μmol of ERY, the same amount of antibiotic than in the ESD, is then investigated. Since in these experiments the amount of ERY to be added in the formulations prior to freeze-drying is low, the addition of ERY was done after suspensions of CS/ChS complexes are formed in comparable conditions, following the method 1 described in the experimental section. The apparent size and zeta potential of all the final colloidal suspensions containing different concentration of ERY was almost equivalent, falling in the ranges of 281 ± 4.8 nm and 37.2 ± 0.5 mV, respectively. Aerogels of 5, 12, and 30 mm of diameter containing 0.02 μmol of ERY showed zones of inhibition smaller than that produced by the ESD, as can be seen in Fig. 7 (see Fig. 5 for the ESD positive control). The values of the IZD were 26 ± 3 mm for the positive control, 15 ± 2 and 18 ± 1 mm for the aerogels of 5 and 12 mm, respectively, while no inhibition zone was found beyond the limits of the aerogel of 30 mm (n = 3). The lack of IZD beyond the limits of the aerogel for the larger material could be explained in terms of the higher retention of ERY within the aerogel related to the presence of a significant higher amount of polysaccharides.

These results indicate, then, a slower diffusion of ERY from the aerogels than from the ESD, probably due to attractive interactions with the polymeric components of the material. New tests were then performed with aerogels of 12 mm loaded with increasing amounts of ERY. In order not to significantly dilute the CS/ChS polyelectrolyte complex suspensions, the method 2 described in the experimental section was applied for the fabrication of the solid materials. The fabricated aerogels produced increasing IZD as the amount of ERY increased, achieving IZD values similar to the ESD when containing an amount of ERY one order of magnitude higher than the ESD, as can be seen in Fig. 8. These results highlight the potential of ERY-loaded CS/ChS-based aerogels as controlled release materials, as the loads of ERY, and concomitantly the diffusion of the antibiotic from the materials, can be modulated.

The interaction of ERY with the polymeric components of the aerogels may produce a release of the antibiotic controlled by equilibrium forces. In this sense, the release of the antibiotic from the materials should be a function of the relative amount of the antibiotic versus the amount of polysaccharides (in mol of ionizable groups). In order to corroborate this hypothesis, aerogels were fabricated keeping constant this magnitude. Aerogels of 5 mm of diameter containing 0.02 μmol of ERY, the same amount than in the ESD of 6 mm, presented a relative amount of ERY of 0.023 mol of ERY/mol of polymeric ionizable groups, so that, aerogels of 5, 12, and 30 mm of diameter have been fabricated containing ERY at a relative amount of 0.023 mol of ERY/mol of polymeric ionizable groups. The results of the corresponding susceptibility tests can be seen in Fig. 7 (for aerogels of 5 mm of diameter), and Fig. 9 (for aerogels of 12 and 30 mm). It was found that the diffusion of ERY from the edge of the aerogels was similar when their relative amount was similar, producing inhibition of bacteria growth at similar distances taking a value around 5 mm, as can be read in Table 2. This is related to the ability of a certain mass of the polymers in the polymeric matrix to retain a certain mass of the antibiotic, according to equilibrium interactions, so that the materials allow controlling the diffusion of the antibiotic in agar media.

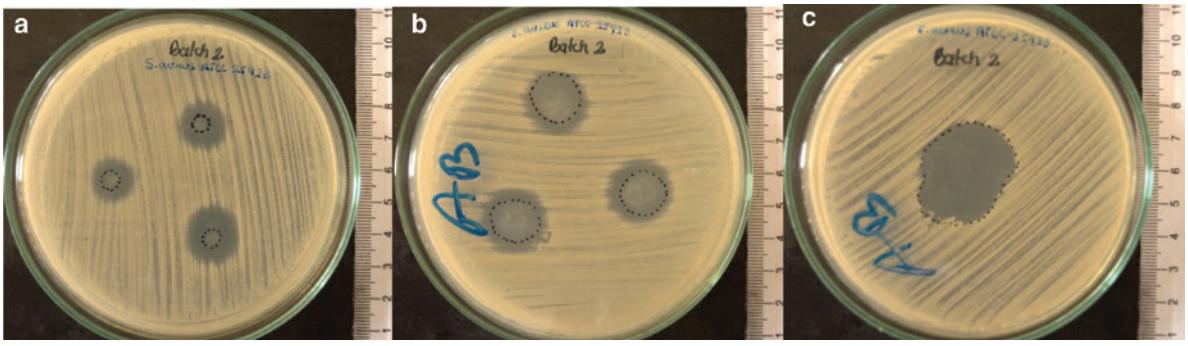

Fig. 7: Susceptibility test of aerogels of 5 (a), 12 (b), and 30 (c) mm of diameter, containing 0.02 μmol of ERY on ATCC 25923 standard *S. aureus* strain.

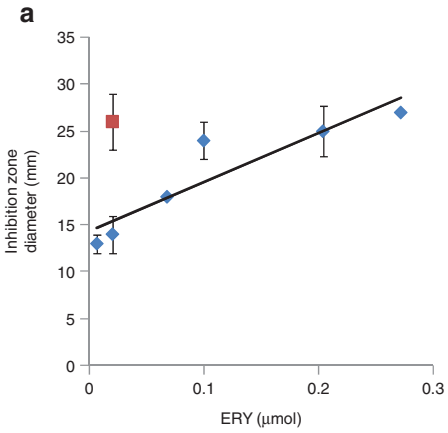

Fig. 8: IZD (mm) produced by aerogels of 12 mm of diameter (♦) and by the ESD (■) as a function of the amount of ERY (n = 3) in cultures of ATCC 25923 standard *S. aureus* strain.

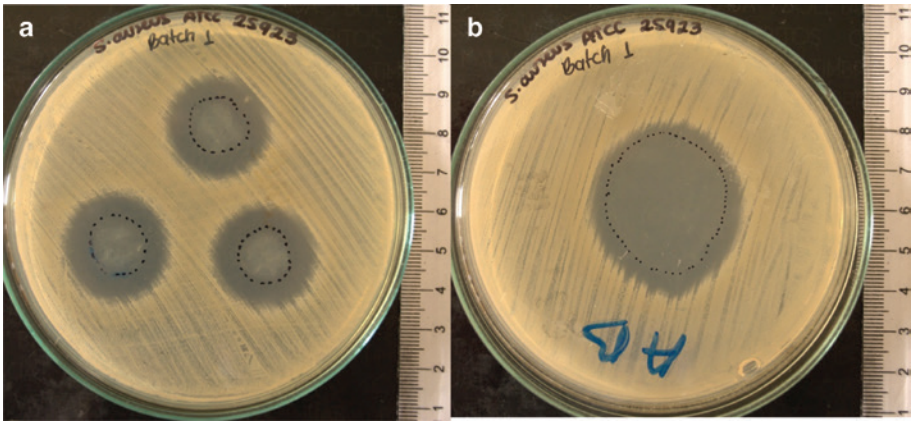

Fig. 9: Susceptibility test of aerogels of 12 (a) and 30 (b) mm of diameter containing a relative amount of ERY of 0.023 (mol of ERY/mol of polymeric charges) on ATCC 25923 standard *S. aureus* strain.

Table 2: Inhibition length from the edge of the aerogels containing ERY at a relative amount of 0.023 (mol/mol of polymeric charges) on cultures of ATCC 25923 standard *S. aureus* strain.

Aerogel diameter (mm)	ERY amount (µmol)	ERY relative density (mol of ERY/mole of polymeric charges)	Inhibition length from the edge (n = 3) (mm)
5	0.02	0.023	5 ± 1
12	0.2	0.023	6 ± 1
30	0.4	0.023	5 ± 1

On the other hand, when a MRSA strain was tested, the antibiotic diffused from the aerogels containing the same relative amount of ERY (0.023 mol of ERY/mol polymeric ionizable groups) or from the ESD (Fig. 5) did not produce inhibition of the bacterial growth, as can be seen in Fig. 10, but, as expected, produced inhibition on the area occupied by the materials.

Aerogels loaded with elephant garlic extract

Resistance to ERY by *Streptoccocus* and *Staphylococcus* genera has been described, associated to target-site modification and active-drug efflux mechanisms [38]. Fatality of *S. aureus* infections is associated to their high

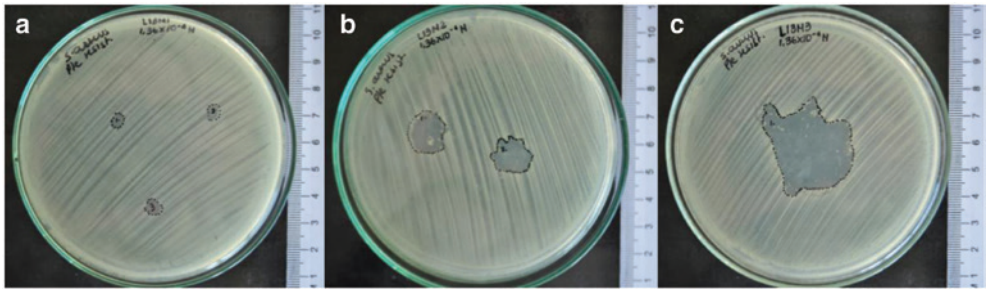

Fig. 10: Susceptibility test of aerogels of 5 (a), 12 (b), and 30 (c) mm of diameter containing a relative amount of ERY with respect to the polymers of 0.023 mol of ERY/mol of polymeric charges on MRSA strain.

resistance to beta-lactamic antibiotics. The emergence of drug resistance among several pathogenic bacteria species jeopardizes the therapeutic effectiveness of antibiotics. However, therapeutic options against pathogens like MRSA can be developed using plants and herbal natural components that may act as non-specific biocides, minimizing the appearance of resistance [39]. Natural extracts of elephant garlic were obtained in cold water, the pH carefully adjusted to 5.0, and then ultrafiltered in order to achieve a pure soluble fraction, removing floccules and large particles. Preliminar experiments show that the minimum inhibitory concentration of the extract was approximately 5 % (v/v). Then the extract at this concentration was added to the container containing CS/ChS nanoparticles produced at different molar ratios in order to explore the formation of colloidal suspensions and measure apparent particle size and zeta potential. The results can be seen in Fig. 11. It can be noticed that in the absence of the natural extract CS/ChS nanoparticles are formed in the whole range of X_{ChS} studied, and an inversion on the zeta potential is produced at X_{ChS} around 0.55. However, in the presence of the elephant garlic extract, particles of around 300 nm of diameter (size PDI in the range of 0.24–0.39) are formed, and macroprecipitation was observed near the electroneutralization point. This occurred at a X_{ChS} of around 0.48, as can be deduced by the inversion of the zeta potential.

In order to produce the aerogels from nanoparticles with absolute values of zeta potential higher than 30 mV, that ensures stability of the nanosystems, a composition of CS/ChS 0.75:1, corresponding to a X_{ChS} of 0.57 is selected. STEM images of nanoparticles performed at this polysaccharide molar ratio and 4.66 % of elephant garlic extract shows spherical particles of around 200 nm, as can be seen in Fig. 2c, slightly smaller than when observed by DLS.

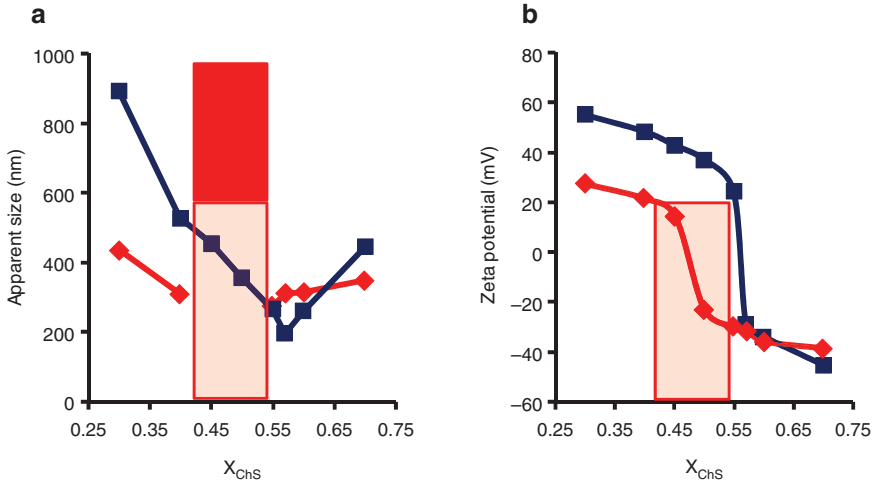

Fig. 11: Apparent hydrodynamic diameter (a) and zeta potential (b) of colloidal suspensions of CS/ChS nanoparticles produced at pH 5.0: (■) pristine; (◆) containing 5 % of elephant garlic extract. Shaded area corresponds to appearance of macroprecipitates in the presence of the extract.

Solid materials of different dimensions were then produced, adding volumes of the CS/ChS colloidal suspension obtained at X_{ChS} of 0.57 and pH 5.0 and containing elephant garlic extract to wells of different size, so that the absolute amount of added extract was 70 µL for each sample. The dry weight of the 70 µL of the extract is approximately 7.5 mg. After freeze-drying the mixtures, solid materials of diameters of 7, 14 and 30 mm of diameter are obtained. The relative weight of the extract in the materials represents 98, 82, and 66 %, respectively. Related to the significant increase in matter of the aerogels, an increase on the E_{app} is observed and for aerogels of 14 mm of diameter, an E_{app} of 6.8 kPa was found, while the corresponding hardness at 40 % deformation was around 14 g. Considering the same approximations and methodology used for the calculation of the porosity in the above reported aerogels, porosity higher than 95 % was found for the aerogel of 7 mm of diameter, and higher than 98 % for the aerogels of 14 and 30 mm of diameter. In addition, the materials showed a tendency to shrink in contact to the air, probably due to atmospheric moisture. This tendency was lower for the materials of 7 mm of diameter, containing the highest relative amount of garlic extract. The materials of 14 mm of diameter shrank both in the x/y plane and in the z axis, and materials of 30 mm, containing the lower relative amount of extract, shrank more appreciably in the z axis, as can be seen in Fig. 3d. This behavior may be due to the presence of amphiphilic molecules in the elephant garlic extract. SEM images shown in Fig. 4c reveal denser materials with thicker and texturized microsheets.

The antibacterial activity of the aerogels containing 7.5 mg of garlic extract is then investigated. It was found that the garlic extract diffuses from the aerogels, and IZD of 33 ± 1 mm have been found for control experiments and experiments performed with aerogels of 7 and 14 mm of diameter, while 37 ± 2 mm for aerogels of 30 mm of diameter, both in cultures of ATCC 25923 and MRSA strains, as can be seen in Fig. 12, highlighting the efficacy of natural extracts against recurrent infections produced by resistant bacterial strains such as MRSA. By contrast to the case of ERY, the diffusion kinetics of the active components does not strongly depend on the amount of the polysaccharides CS and ChS in the formulation. This may be due to a weak interaction between the polysaccharides and the active components, related to a lack of net charge on their structure, as in the case of allicin, and to the higher mass of extract relative to the mass of polysaccharides.

Final remarks

CS/ChS ultralight aerogels are materials with high potential in wound healing of chronic wounds such as diabetic foot and venous ulcers, and, applied to the skin lesions, they improve the quality of the dermal tissue,

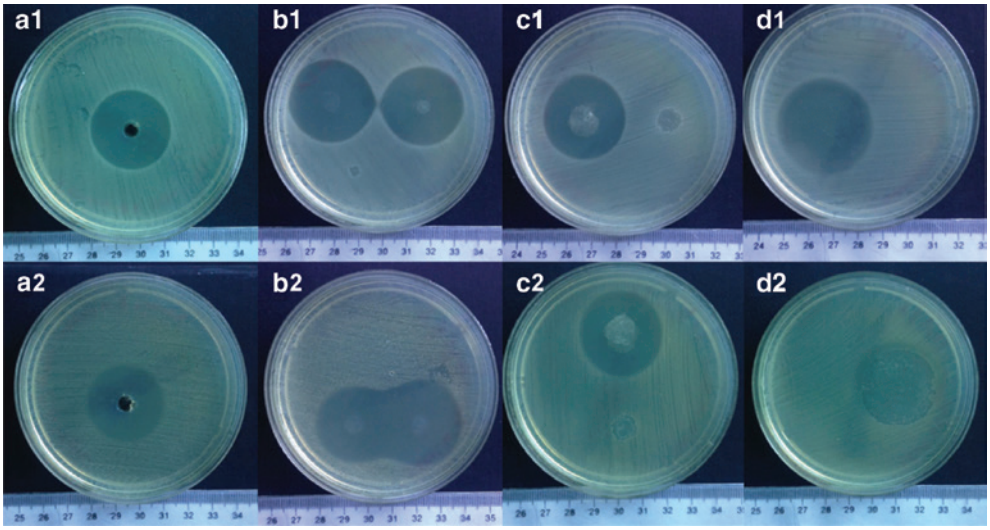

Fig. 12: Susceptibility test of 70 µL of elephant garlic extract (positive control, a1 and a2), and aerogels containing of 7.5 mg of dry elephant garlic extract of 7 (b1 and b2), 14 (c1 and c2) and 30 mm (d1 and d2) of diameter against ATCC 25923 (entries 1) and MRSA (entries 2).

with suppression of pain and bad smell, accelerating wound healing in these chronic ulcers, as has been previously corroborated [21]. Its production is simple, avoiding chemical reactions or the use of organic solvents. The materials are light and soft, and their mechanical properties facilitate their application in open wounds, easily adapting to the wound contour. In addition, they can be easily compressed and packed in sterile containers, thus facilitating their storage and transport, conditions necessary for its adequate commercialization and clinical management. After applied in the open wound, the material swallows and hydrates, so that it does not need to be removed after application, since is physiologically metabolized. The low density of the materials helps avoiding adverse reactions. The therapeutic potential of these materials, based on their angiogenic properties [21], is enhanced by the antibacterial action found in this study against *S. aureus*, a recurrent pathogenic microorganism in chronic skin lesions. This antibacterial action is also presented against MRSA.

We have also proven the ability of the material to incorporate variable amounts of the antibiotic ERY, and release it in MHA plates, observing growth inhibition of sensitive *S. aureus*. The incorporation of ERY to CS/ChS-based aerogels may constitute an additional means of enhancement of the therapeutic benefits of the solid material, helping avoiding and fighting infection of skin lesions, by releasing a desired amount of the antibiotic. Once applied in the open wound and the material hydrates, the antibiotic may diffuse to the environment with kinetics controlled by equilibrium interactions with the material components. The dosage of the antibiotic is easily tuned, according to the method of fabrication described here, that involves the formation of the interpolymer nanocomplexes prior to the addition of the antibiotic.

On the other hand, and regarding the inconvenience of potential selective resistance, the materials also allow the incorporation of elephant garlic extract (as well as potentially a number of other active extracts from plants) that also showed antibacterial activity against both sensitive and MRSA strains of *S. aureus*. The active components of the extract do not seem to strongly interact with the aerogel polysaccharide components, so that their diffusion kinetics are a function of their absolute content rather than of the content relative to the polysaccharide mass, as in the case of ERY.

The obtained results reveal, thus, the potential of these materials as carriers of bioactive molecules for topic uses. Apart from chronic wounds such as diabetic foot and venous ulcers, ERY and elephant garlic extract-loaded CS/ChS-based aerogels could be applied to other infected skin lesions such as bedsores, dermatitis, skin abscesses, and cellulitis.

Conclusions

CS/ChS-based aerogels of around 5, 12, and 30 mm of diameter have been fabricated, unloaded, and loaded with ERY and with elephant garlic extract. As a first step of fabrication, colloidal suspensions containing CS/ChS nanocomplexes and eventually other added additives, such as the antibiotic or the natural extract, have been formed avoiding formation of macroprecipitates. The solid materials arising after solvent removal by freeze-drying the colloidal suspensions present a porous structure consisting of a network of microfibers and microsheets. Pristine aerogels showed smooth surface on the microfibers and microsheets, hardness of around 12 g at 40 % deformation, E_{app} of around 2 kPa, porosity higher than 99 %, and activity against sensitive *S. aureus* as well as against MRSA. The inclusion of ERY produced the appearance of deposits and crystals on the microfibers and microsheets, a decrease on the hardness (5.4 g at 40 % deformation) and E_{app} (1.4 kPa), similar porosity than that of the pristine aerogels, and activity against sensitive *S. aureus* beyond the limits of the aerogels in agar culture media, but not against MRSA. The diffusion of the antibiotic was controlled by equilibrium forces with the polymeric components of the aerogels, which allowed controlling the release. The incorporation of elephant garlic extract produced texturization and thickening of the microfibers and microsheets, an increase on the hardness with respect to that of the pristine aerogels (around 14 g at 40 % deformation) and E_{app} (6.8 kPa), porosity higher than 95 %, and activity against both sensitive *S. aureus* and MRSA strains beyond the limits of the aerogels. The diffusion of the active components of the extract did not depend on the mass of polysaccharides of the aerogels, revealing a weak interaction. The therapeutic

potential of the aerogels in wound healing is enhanced by the antibacterial action found in this study against *S. aureus*, a recurrent pathogenic microorganism in chronic skin lesions. This antibacterial action is also presented against MRSA, and important strain responsible for nosocomial infections in hospitals. Their activity against MRSA of pristine aerogels can be reinforced by the addition of elephant garlic extract, which is easily released from the aerogels in culture medium at therapeutic concentrations.

Acknowledgments: This work was supported by Fondecyt Regular (grant no. 1150899, 1161450, and 1171118), Fondecyt Iniciación (grant no. 11150919), CONICYT-FONDAP 15130011, and *Gobierno Regional de Los Ríos* (grants FIC-R-2011 and FIC-R 2012-117).

References

[1] F. Oyarzun-Ampuero, A. Vidal, M. Concha, J. Morales, S. L. Orellana, I. Moreno-Villoslada. *Curr. Pharm. Des.* **21**, 4329 (2015).
[2] B. S. Anisha, D. Sankar, A. Mohandas, K. P. Chennazhi, S. V. Nair, R. Jayakumar. *Carbohydr. Polym.* **92**, 1470 (2013).
[3] S.-N. Park, H. J. Lee, K. H. Lee, H. Suh. *Biomaterials* **24**, 1631 (2003).
[4] R. Jayakumar, M. Prabaharan, P. T. Sudheesh Kumar, S. V. Nair, H. Tamura. *Biotechnol. Adv.* **29**, 322 (2011).
[5] V. Bermejo, L. Spadaccini, G. R. Elbert, A. I. E. Duarte, M. Erbin, P. Cahn. *Medicina (B. Aires)* **72**, 283 (2012).
[6] D. A. Talan, A. Krishnadasan, R. J. Gorwitz, G. E. Fosheim, B. Limbago, V. Albrecht, G. J. Moran. *Clin. Infect. Dis.* **53**, 144 (2011).
[7] F. Salgado Ordóñez, A. Arroyo Nieto, A. B. Lozano Serrano, A. Hidalgo Conde, J. Verdugo Carballeda. *Med. Clin.* **133**, 552 (2009).
[8] M. Raya-Cruz, I. Ferullo, M. Arrizabalaga-Asenjo, A. Nadal-Nadal, M. P. Díaz-Antolín, M. Garau-Colom, A. Payeras-Cifre. *Enferm. Infecc. Microbiol. Clin.* **32**, 152 (2014).
[9] E. S. Yang, J. Tan, S. Eells, G. Rieg, G. Tagudar, L. G. Miller. *Clin. Microbiol. Infect.* **16**, 425 (2010).
[10] J. A. Bustos-Martínez, A. Hamdan-Partida, M. Gutiérrez-Cárdenas, X. México. *Rev. Biomed.* **17**, 287 (2006).
[11] L. B. Sandrea Toledo, P. Reyes, E. Josefina, A. Paz Montes, E. L. Torres Urdaneta. *Rev. Soc. Venez. Microbiol* **32**, 88 (2012).
[12] M. S. Dryden. *J. Antimicrob. Chemother.* **65**, iii35 (2010).
[13] C. Merritt, J. Haran, J. Mintzer, J. Stricker, R. Merchant. *BMC Emerg. Med.* **13**, 26 (2013).
[14] F.-F. Gu, Q. Hou, H.-H. Yang, Y.-Q. Zhu, X.-K. Guo, Y.-X. Ni, L.-Z. Han. *PlosOne* **10**, e0123557 (2015).
[15] B. C. Herold, L. C. Immergluck, M. C. Maranan, D. S. Lauderdale, R. E. Gaskin, S. Boyle-Vavra, C. D. Leitch, R. S. Daum. *J. Am. Med. Assoc.* **279**, 593 (1998).
[16] M. Otto. *Int. J. Med. Microbiol.* **303**, 324 (2013).
[17] B. Casado-Verrier, C. Gómez-Fernández, J. R. Pano-Pardo, R. Gómez-Gil, J. Mingorance-Cruz, R. M.-A. de Celada, P. Herranz-Pinto. *Enferm. Infecc. Microbiol. Clin.* **30**, 300 (2012).
[18] A. E. Nel, L. Madler, D. Velegol, T. Xia, E. M. V. Hoek, P. Somasundaran, F. Klaessig, V. Castranova, M. Thompson. *Nat. Mater.* **8**, 543 (2009).
[19] T. Koike, T. Izumikawa, J.-I. Tamura, H. Kitagawa. *Biochem. Biophys. Res. Commun.* **420**, 523 (2012).
[20] J. S. Park, H. J. Yang, D. G. Woo, H. N. Yang, K. Na, K. H. Park. *J. Biomed. Mater. Res. Part A* **92**, 806 (2010).
[21] A. Vidal, A. Giacaman, F. A. Oyarzun-Ampuero, S. Orellana, I. Aburto, M. F. Pavicic, A. Sánchez, C. López, C. Morales, M. Caro, I. Moreno-Villoslada, M. Concha. *Am. J. Ther.* **20**, 394 (2013).
[22] S. Ankri, D. Mirelman. *Microb. Infect.* **1**, 125 (1999).
[23] A. W. Bauer, W. M. Kirby, J. C. Sherris, M. Turck. *Am. J. Clin. Pathol.* **45**, 493 (1966).
[24] B. J. Frisken. *Appl. Opt.* **40**, 4087 (2001).
[25] P. Prati, C. M. Henrique, A. S. D. Souza, V. S. N. D. Silva, M. T. B. Pacheco. *Food Sci. Technol. (Campinas)* **34**, 623 (2014).
[26] P. Canizares, I. Gracia, L. A. Gomez, A. Garcia, C. Martin De Argila, D. Boixeda, L. de Rafael. *Biotechnol. Prog.* **20**, 32 (2004).
[27] A. Bauer, W. Kirby, J. C. Sherris, M. Turck. *Am. J. Clin. Pathol.* **45**, 493 (1966).
[28] F. R. Cockerill. *Performance Standards for Antimicrobial Susceptibility Testing: Twenty-Third Informational Supplement;[... provides updated tables for... M02-A11, M07-A9, and M11-A8]*. Clinical and Laboratory Standards Institute, Wayne, PA, USA (2013).
[29] A. Espinel-Ingroff, T. M. Kerkering, P. R. Goldson, S. Shadomy. *J. Clin. Microbiol.* **29**, 1089 (1991).
[30] S. L. Orellana, A. Giacaman, A. Vidal, C. Morales, F. Oyarzun-Ampuero, J. G. Lisoni, C. Henríquez-Báez, L. Morán-Trujillo, M. Concha, I. Moreno-Villoslada. *Pure Appl. Chem.* **90**, 901 (2018).
[31] M. C. Gutiérrez, M. L. Ferrer, F. del Monte. *Chem. Mater.* **20**, 634 (2008).
[32] X. Zhang, C. Li, Y. Luo. *Langmuir* **27**, 1915 (2011).
[33] L. Sanhueza, J. Castro, E. Urzúa, L. Barrientos, F. Oyarzun-Ampuero, H. Pesenti, T. Shibue, N. Sugimura, W. Tomita, H. Nishide, I. Moreno-Villoslada. *J. Phys. Chem. B* **119**, 13208 (2015).

[34] M. S. Benhabiles, R. Salah, H. Lounici, N. Drouiche, M. F. A. Goosen, N. Mameri. *Food Hydrocoll.* **29**, 48 (2012).
[35] M. Kong, X. G. Chen, K. Xing, H. J. Park. *Int. J. Food Microbiol.* **144**, 51 (2010).
[36] F. K. Tavaria, E. M. Costa, E. J. Gens, F. X. Malcata, M. E. Pintado. *J. Dermatol.* **40**, 1014 (2013).
[37] L. Hernandez-Ochoa, A. Gonzales-Gonzales, N. Gutierrez-Mendez, L. Munoz-Castellanos, A. Quintero-Ramos. *Rev. Mex. Ing. Quim.* **10**, 455 (2011).
[38] P. Tang, D. E. Low, S. Atkinson, K. Pike, A. Ashi-Sulaiman, A. Simor, S. Richardson, B. M. Willey. *J. Clin. Microbiol.* **41**, 4823 (2003).
[39] A. Kali. *Pharmacogn. Rev.* **9**, 29 (2015).